FINE WAVELENGTH ID FOR TUNABLE LASER LOCAL OSCILLATORS*

M.G. Savage and R.C. Augeri

Eaton Corporation AIL Division, Melville, New York 11747

SUMMARY

This paper describes a wavelength ID device which consists of an electronic servo-controlled Fabry-Perot etalon. Measurements performed with a CO_2 laser show that the etalon has a finesse $F > 30$ which is maintainable for several days. These tests also demonstrate that the etalon system is capable of resonance frequency stability $\frac{\Delta\nu}{\nu} \simeq 2 \times 10^{-7}$ during similar time periods. With currently available mirror coatings, this level of performance is achievable over an optical bandwidth $\Delta\lambda = 3$ μm centered at $\lambda = 10$ μm.

INTRODUCTION

With the increased concern about possible damage to the atmosphere by chemical pollution, much interest has arisen in the chemistry of the stratosphere. Several important constituents which are present in only trace amounts, such as ozone O_3 (reference 1), chlorine monoxide ClO (references 2 and 3), and the various chlorofluorocarbons (reference 4) have prominent absorption-emission spectra in the 8 to 12 μm wavelength region. Remote sensing of these and many other gases can be accomplished with infrared heterodyne spectrometers using tunable diode lasers (TDL) as local oscillators (LO) (references 5 and 6).

TDL's exhibit narrow spectral emission widths which are piecewise-continuously tunable over more than 100 wavenumbers (references 7, 8, 9, and 10). While such tunability greatly increases the spectral coverage obtainable with a single-TDL spectrometer, it introduces a degree of uncertainty in the LO frequency which is not present when a low-pressure gas laser is used. In studies of spectrally narrow features such as stratospheric gas absorption lines, this LO frequency uncertainty can have serious effects on measurement accuracy (reference 11). It is often necessary to determine the LO frequency with a resolution $\frac{\Delta\nu}{\nu} = 1.8 \times 10^{-7}$ (about 5 MHz at $\lambda = 10.6$ μm).

*This work was supported by NASA, Langley Research Center, Hampton, Virginia 23665.

WAVELENGTH ID TECHNIQUES

Measurements of TDL output parameters such as wavelength versus drive current have generally shown large temporal variability rendering wavelength ID via drive current calibration nearly useless (references 7 and 10). A successful means of accurate wavelength determination will rely as little as possible on the stability of the TDL.

The use of a reference gas absorption cell is capable of providing the necessary wavelength resolution if a suitable absorber can be found. (It is generally impossible to use the target gas line as a reference because of the conflicting requirements of a low absorption coefficient for viewing through kilometers of atmosphere and a high absorption coefficient for viewing through centimeters of test cell.) To be used successfully, the absorption spectrum of the reference gas must be determined with the same resolution as that desired of the TDL's wavelength. Since there are many atmospheric gases of interest, high resolution spectra of many potential reference absorbers must be generated. In addition, some knowledge of the TDL's wavelength-current tuning rate is required by this technique because it is unlikely that the reference line frequency will exactly coincide with the target line frequency. The larger this separation is, the higher the accuracy with which the TDL's tuning rate must be known to maintain a given level of LO frequency accuracy. Also, the above calibration technique relies on an ageless TDL whose tuning parameters do not change.

Another technique which is capable of providing the desired wavelength ID accuracy uses a wideband detector such as a metal-oxide-metal (MOM) diode to mix the outputs of a TDL and a stabilized low-pressure gas laser. The resultant heterodyne beat note can be measured with very high precision. MOM diodes designed for operation near λ = 10 μm can have IF bandwidths in excess of 30 GHz (1 cm^{-1}) allowing continuous coverage of the spectral intervals between CO_2 laser lines (reference 12). While these detectors do not have the necessary sensitivity to perform the desired atmospheric measurements, they are well suited to the wavelength ID function. This technique is limited, however, to those spectral regions where suitable gas laser oscillators are available.

Another device capable of high wavelength resolution is the Fabry-Perot etalon (FPE), which is an optically resonant cavity formed by two parallel plane partial reflectors. Mirror coatings presently available can allow an FPE to operate with a finesse $F \geq 30$ throughout a spectral interval $\Delta\lambda \simeq 3$ μm near λ = 10 μm. Until recently these devices were not stable enough to permit their potentially high resolution to be used for TDL wavelength calibration. An etalon has been designed and constructed which overcomes these stability problems, maintaining a finesse $F = 33 \pm 3$ for a period of 2 days, and showing resonance frequency stability of $\pm$10 MHz over 4 hours. The design is capable of even longer term stability.

HIGH RESOLUTION TUNABLE FPE

The etalon employs a capacitance-bridge servo technique to maintain mirror parallelism and to provide continuous passband tuning (references 13, 14, and 15). The FPE uniquely uses a Cer-Vit mirror spacer as the primary length standard for the optical cavity. (Cer-Vit is manufactured by Owens-Corning Fiberglas Corporation.) The thermal stability of the spacer reduces the need for precise temperature control of the etalon to a manageable level. The mirrors which form the optical cavity are attached to piezoelectric elements (PZT) which can accurately vary the cavity length and, therefore, spectrally tune the etalon.

The mirrors, which form the etalon shown schematically in Figure 1, consist of multilayer dielectric coatings deposited on 5-cm-diameter ZnSe substrates. They have a reflectivity $R \geq 0.90$ over the spectral interval $8.9\ \mu m \leq \lambda \leq 11.2\ \mu m$. The substrates are antireflection coated on one side and have small wedge angles. The plates are matched in flatness to better than $\lambda/175$ at $\lambda = 10.6\ \mu m$. The spacer is a 4-cm-long cylinder whose surfaces were ground flat and parallel to nearly $\lambda/1000$ at $\lambda = 10.6\ \mu m$.

Gold has been sputtered onto the mirror and spacer surfaces in a pattern shown in Figure 2. When the mirrors are positioned close to the spacer, the opposing gold pads form parallel plate capacitors. The pads on the spacer are slightly oversized to facilitate mirror-spacer alignment. The gaps between the mirrors and the spacer are manually preset to a nominal 50 μm.

Each mirror of the FPE is independently controlled by an electronic servo mechanism. The two pairs of orthogonal capacitors, arbitrarily designated $X_1 - X_2$ and $Y_1 - Y_2$, are used to maintain mirror-spacer parallelism, thereby also assuring mirror-mirror parallelism. This is accomplished by balancing the pairs in separate capacitance bridges. As the mirrors drift out of parallel, the resulting bridge voltages are sensed and used to drive the PZT's supporting the mirrors. Cavity length control and therefore resonance frequency control is performed by balancing the two unpaired Z-capacitors against fixed-value reference capacitors in two other bridges. The frequency stability of the etalon is dependent on the stability of the fixed reference capacitors and the Cer-Vit spacer.

Since the FPE mirrors are individually controlled, six high-resolution capacitance bridges are required to form the servo system. A block diagram of the electronics used to control one of the mirrors is shown in Figure 3 (reference 13). Each of the three bridges has a balance control to compensate for stray capacitances arising from either the etalon structure or the servo itself. Spectral tuning of the FPE is accomplished by combining the output of the Z-bridge with an adjustable offset voltage; the combination then is used to drive the PZT's. This tuning method is readily adaptable to digital control and allows continuous spectral coverage within limits set by the maximum PZT motion.

Changes in the pad gap ℓ are related to changes in the capacitance C according to the expression:

$$\frac{d\ell}{\ell} = \frac{dC}{C} \tag{1}$$

(Equation (1) assumes that there is a negligible area difference between the pairs of capacitors.) Also, changes in the cavity length L are related to changes in the pad gaps by:

$$d\ell = 1/2\ dL \tag{2}$$

The factor of 1/2 arises when both plates are translated by the same distance dL. For one plate fixed, the relation reduces to $d\ell = dL$. To achieve the desired wavelength resolution of 1.8×10^{-7}, it can be shown from the etalon resonance condition that:

$$\frac{dC}{C} = 9 \times 10^{-8} \frac{L}{\ell} \tag{3}$$

For the case in which L = 4 cm and ℓ = 50 μm, the necessary capacitance bridge resolution corresponding to an FPE resonance frequency resolution of 5 MHz at λ = 10.6 μm is $\frac{dC}{C} = 7.2 \times 10^{-5}$.

Stabilization of an FPE with such high precision requires special consideration of temperature and pressure effects. Since the spacer is the length standard of the cavity, it must be dimensionally stable to the same degree as the desired frequency resolution. Since Cer-Vit has an expansion coefficient of $0.12 \times \frac{10^{-6}\text{cm}}{\text{cm}^{\circ}\text{C}}$, temperature stability of about 1.5°C is necessary to achieve the desired result. This etalon is mounted in a vacuum chamber to eliminate the effects of atmospheric pressure variations on the dielectric constant of the capacitor gaps and the index of refraction of the air between the mirrors.

Measured Performance

The measurements of the FPE finesse and frequency stability at λ = 10.6 μm were performed using the setup shown in Figure 4. The collimated output of the HeNe laser was directed through the etalon to a pyroelectric detector. As the spacing between the mirrors is varied by the PZT's, peaks in the output of the detector occur which correspond to cavity length changes of $\lambda/2$ or 0.3164 μm. The voltage expansion coefficient of the PZT's is then easily calculated.

Because the mirrors are not optimized for operation at visible wavelengths, the peaks that are observed are not very sharp, introducing an error of about 10 percent into the measurement of the expansion coefficient. The output of a waveguide CO_2 laser operating at $\lambda = 10.588$ μm was then directed through the etalon with an FPE passband tuned across the laser output by PZT voltage adjustment. The measured transmission versus length change can be used to estimate the finesse because the cavity length is known. Figure 5 shows two curves of calculated passband shape for two values of finesse and PZT expansion coefficient. Also shown are data points measured on two occasions two days apart.

The measurement of the frequency stability of the FPE was performed using the same optical setup by tuning the FPE so that a half-transmission point of a passband overlapped the CO_2 laser output. The detected laser power transmitted by the etalon was monitored by a strip-chart recorder. Adjusting the FPE to a passband skirt increases its frequency discrimination. The long-term frequency stability of the laser is believed to be better than 3 MHz and its output power was continuously monitored. The FPE was mounted in a vacuum chamber, but its temperature was not actively controlled.

Figure 6 shows the measured resonance frequency stability of the etalon. The dashed curve shows that the frequency deviation was less than 10 MHz over a period of 4 hours in the early afternoon. The solid curve shows a continuous drift through the evening. This drift is caused by a decrease in ceramic reference capacitor temperature as the ambient lab air cooled. Measurements of spacer temperature during this period indicated a stability of better than $1^{\circ}C$. The figure clearly shows that the FPE is spectrally stable to an unprecedented degree provided sufficient reference capacitor thermal stability is achieved. An improved air gap reference is being developed.

WAVELENGTH ID WITH AN FPE

The schematic diagram of a possible TDL wavelength calibration system using a high-resolution FPE is shown in Figure 7. The output of a TDL is first prefiltered to isolate a single frequency mode. Part of this power is directed through the FPE to a detector whose output is then fed back to control the TDL temperature or drive current. Depending on the available TDL power, FPE parameters, and calibration detector sensitivity, it may be necessary to impress a slight frequency modulation on the TDL output to enhance calibration accuracy. This modulation would have no significant effect on the laser's performance as an LO.

It is absolutely necessary to prefilter the TDL output; this can be done with a small monochromator. The removal of extraneous TDL frequency modes is required by the spectrometer to avoid modal self-beating effects and possible IF ambiguity (reference 10). The bandpass of this monochromator can be as large as a TDL mode width ($\sim 1\ cm^{-1}$), if necessary, but some additional filtering may be required in the calibration system to position the TDL output within a particular high-resolution FPE passband.

High-finesse, long-cavity etalons need special attention for their beam quality requirements. Both beam divergence and variations of angle of incidence must be minimized to extract the best FPE system performance. For the etalon previously described, the beam divergence half-angle should be less than a few tenths of a degree to avoid excessive resonance frequency shifts and finesse degradation. Since the etalon is used at normal incidence, its sensitivity to changes in incidence angle is somewhat reduced, but these changes should still be kept below several tenths of a degree to avoid too much frequency shift.

CONCLUSIONS

For tunable diode lasers to realize their potential in high-resolution heterodyne spectroscopy, some means of accurately determining their emission frequency is required. In general, characteristics of a TDL are not sufficiently stable over the long term to allow their one-time calibration. Several potential calibration techniques have been discussed which have varying degrees of flexibility and accuracy. Any of these methods could be incorporated into a spectrometer as a subsystem. A Fabry-Perot etalon has been developed which is capable of calibrating a TDL output with a resolution of about 5 MHz at wavelengths near 10 μm and measured data has been presented. This device can form the basis of a highly flexible and accurate wavelength ID system.

REFERENCES

1. R. A. McClatchey, W. S. Benedict, S. A. Clough, D. E. Burch, R. F. Calfee, K. Fox, L. S. Rothman, and J. S. Garing, AFCRL Atmospheric Absorption Line Parameters Compilation, AFCRL-TR-73-0096 (1973).

2. R.T. Menzies, J. S. Margolis, E. D. Hinkley, and R. A. Toth, Appl Opt 16, 523 (1977).

3. R. S. Rogowski, C. H. Bair, W. R. Wade, J. M. Hoell, and G. E. Copeland, Appl Opt 17, 1301 (1978).

4. J. M. Hoell, C. H. Bair, C. Harward, and B. Williams, Geophys Res Lett 12, Dec 1979.

5. M. A. Frerking and D. J. Muehlner, Appl Opt 16, 526 (1977).

6. R. T. Ku and D. L. Spears, IEEE J-QE QE-13, 72D (1977).

7. G. A. Antcliffe and S. G. Parker, J. Appl Phys 44, 4145 (1973).

8. K. J. Linden, K. W. Nill, and J. F. Butler, IEEE J-QE QE-13, 720 (1977).

9. W. Lo, G. P. Montgomery, Jr., and D. E. Swets, J. Appl Phys 47, 267 (1976).

10. M. G. Savage, R. C. Augeri, and B. J. Peyton, NASA Contractor Report 159121.

11. R. K. Seals and B. J. Peyton, Proceedings of the International Conference on Environmental Sensing and Assessment, Vol 1, p 10-4, Sept 1975.

12. A. Sanchez, C. F. Davis, Jr., C. C. Liu, and A. Javan, J. Appl Phys 49, 5270 (1978).

13. T. R. Hicks, N. K. Reay, and R. J. Scadden, J. Phys E: SCI INSTR 7, 27, (1974).

14. T. R. Hicks, N. K. Reay, and C. L. Stephens, Astron and Astrophys 51, 367 (1976).

15. R. V. Jones and J. C. S. Richards, J. Phys E: SCI INSTR 6, 589 (1973).

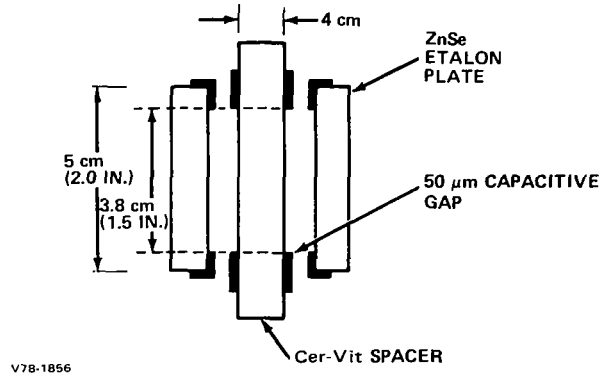

Figure 1.- Fabry-Perot etalon schematic.

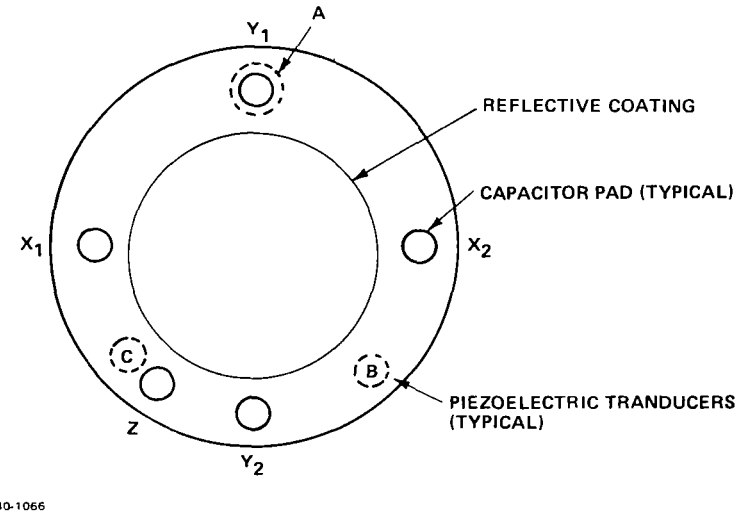

Figure 2.- Plan view of etalon plate showing capacitance pads and piezoelectric transducers.

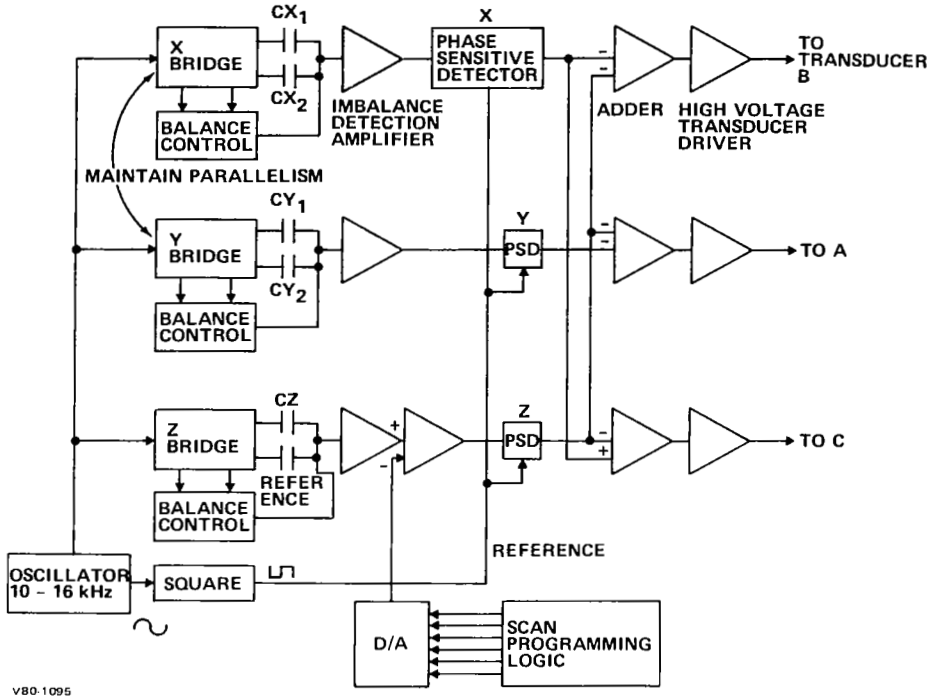

Figure 3.- Capacitance bridge electronics block diagram.

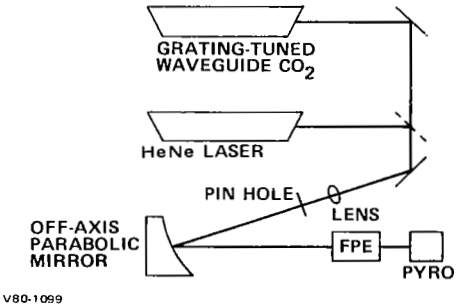

Figure 4.- Optical setup for measurement of FPE finesse and stability.

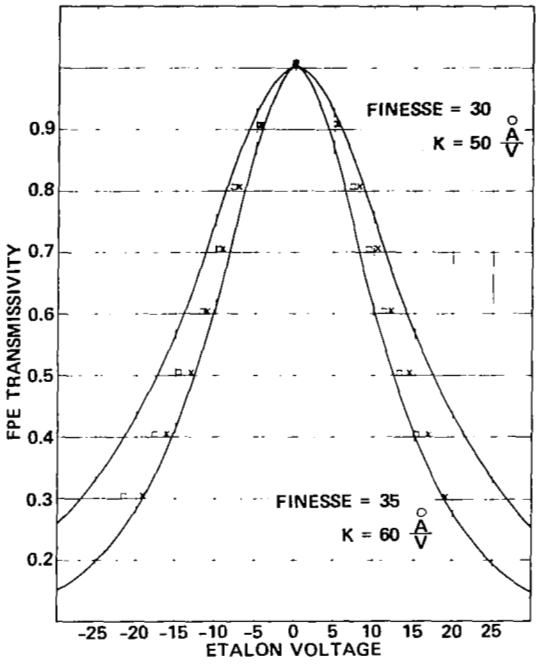

Figure 5.- Measured high-resolution FPE finesse.

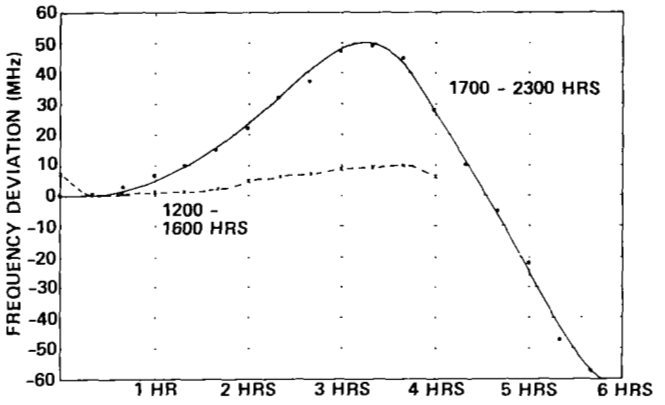

Figure 6.- Measured FPE resonance frequency stability.

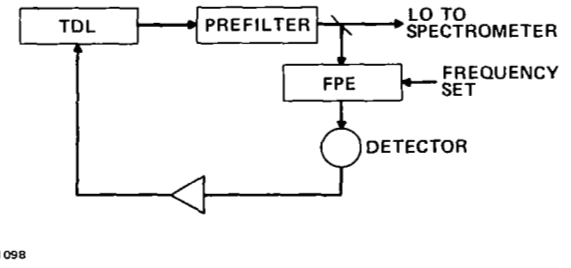

Figure 7.- TDL wavelength ID system.